Chaos, Solitons and Fractals 209 (2026) 118542

Contents lists available at ScienceDirect

Chaos, Solitons and Fractals

journal homepage: www.elsevier.com/locate/chaos

Global population crisis scenarios predicted by a general nonlinear dynamical model

Alessio Zaccone [a,*], Kostya Trachenko [b,1]

[a] Department of Physics "A. Pontremoli", University of Milan, via Celoria 16, 20133 Milan, Italy
[b] School of Physical and Chemical Sciences, Queen Mary University of London, Mile End, London, UK

ARTICLE INFO

Keywords:
Population dynamics
Global population
Mathematical demography
Nonlinear dynamics

ABSTRACT

We show that a simple nonlinear differential equation (originally studied in the physics of disordered systems) mathematically describes key regimes of global population growth over the past 12000 years. Different growth regimes since the early Neolithic until the present can be interpreted within a single nonlinear rate-feedback equation in appropriate limits. These include the well-known Malthus (exponential) and Verhulst (logistic) growth laws, as well as von Foerster-type hyperbolic growth as a controlled low-order truncation. While older models may provide valid fits to limited time intervals, their approximate nature prevents them from being predictive over longer periods of time. The proposed framework provides a compact analytical setting to explore future scenarios, including a deliberately conservative, worst-case illustration in which the global population could halve as early as 2064 if carrying-capacity constraints became abruptly active today.

The first modern attempt to mathematically describe the time evolution of biological populations goes back to Malthus, who identified two central facts which regulate the growth of a population based on the number of its individual elements: birth and death. Assuming a closed population (with no inward or outward fluxes), one can define an average birth rate per element per unit time and an average death rate per element per unit time. This leads to the following equation for the rate of change of the number of elements in the population, y, originally proposed by Malthus in 1798 [1]:

$$\frac{dy}{dt} = b\,y - d\,y = r\,y, \tag{1}$$

where b and d are the birth and death rates per element per unit time, respectively, and $r = b - d$ is known as the productivity of the individual element. If both b and d are constants, so is r, and the solution to Eq. (1) is exponential growth if $b > d$ or exponential decay if $b < d$. In demography, Malthusian growth has often been used to motivate discussions of socioeconomic drivers of fertility rates and long-term sustainability in order to avert potential crises due to overpopulation outrunning resources.

However, soon after Malthus' essay, it became clear that assuming a constant r is too strong, because populations tend to self-regulate based on available resources. This led Verhulst [2] to hypothesize that r decreases with y, and in particular to assume a linear decrease: $r(y) = r_0(1 - y/\kappa)$, where r_0 is a constant and κ is the carrying capacity of the environment. With this correction in Eq. (1), unbounded exponential growth is replaced by a limited growth ending in a stable plateau as $t \to \infty$, producing the logistic curve [3,4].

Taking a different view, von Foerster and co-workers argued [5] that intelligent beings would organize in a strongly linked society, thus reducing the original problem to that of a two-person game between the population and nature as its opponent. Based

* Corresponding author.
E-mail address: alessio.zaccone@unimi.it (A. Zaccone).
[1] Deceased.

https://doi.org/10.1016/j.chaos.2026.118542
Received 27 October 2025; Received in revised form 28 February 2026; Accepted 15 May 2026
Available online 22 May 2026

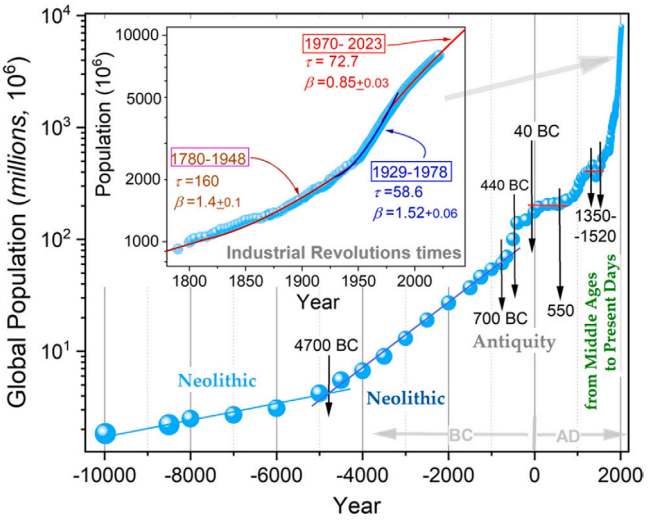

Fig. 1. Evolution of the global population over the past 12,000 years until now. Symbols refer to empirical measurements and continuous lines are the best fits obtained with the functional forms (i)–(iv) discussed in the text. Simple exponential growth is given by straight lines, while long plateaus appear as flat horizontal segments. The inset shows stretched-exponential (SEF) and compressed-exponential (CEF) growth regimes. *Source:* Reproduced from Ref. Sojecka and Drozd-Rzoska [8] under the Creative Commons Attribution 4.0 International License (CC BY 4.0). No changes were made to the original figure.

on this assumption, productivity would increase with y, for example as $r(y) \propto y$. Using the then available global population data, they found an excellent fit with a hyperbolic function $y(t) = A/(D - t)$, corresponding to a Riccati-type equation (see also [6]). It was recognized already in following decades that the global population trend diverged from this prediction, averting the doomsday scenario in 2026.

In addition to classical growth laws, a large literature addresses population crises via scenario-specific extensions of logistic-type models, including formulations with explicit delays, thresholds, or multiple regulatory functionals; see e.g. Perevaryukha [7] and references therein. In contrast, the objective of the present work is to show that several empirically observed growth regimes can be captured by a single analytically tractable nonlinear rate-feedback equation, without introducing explicit time delays or piecewise regulatory mechanisms.

A recent work [8] has shown that the global population evolution over the past 12,000 years has gone through various growth regimes, including short intervals of decline (e.g. Black Death). Excluding these short decline periods, the most prominent regimes, as visible in Fig. 1, can be described phenomenologically by: (i) simple exponential growth (Malthus), corresponding to straight lines in a semi-log plot; (ii) long plateaus $y(t) \approx const$; (iii) stretched-exponential growth (SEF), $\exp\left[(t/\tau)^{\beta}\right]$ with $\beta < 1$; and (iv) compressed-exponential growth (CEF), $\exp\left[(t/\tau)^{\beta}\right]$ with $\beta > 1$. Importantly, in this paper we do not claim that these empirical fit functions are exact closed-form solutions of our nonlinear ODE; rather, we show that the ODE generates the corresponding growth behaviours (curvatures) in controlled limits and over the empirical time windows of interest.

A similar stretched-exponential function, with the sign reversed inside the exponential, $y(t) \sim \exp\left[-(t/\tau)^{\beta}\right]$, has been studied for almost two centuries in physics, at least since Kohlrausch studied the electric discharge of a Leyden jar [9,10]. Since then, stretched-exponential decay (Kohlrausch function) has been observed in countless experiments and simulations of time-dependent phenomena in glasses and other amorphous solids [11–13]. More recently, compressed-exponential decay ($\beta > 1$) has also been detected in metallic glasses [14,15] and colloidal gels [16].

Nonlinear rate-feedback equation

We consider a nonlinear model in which the productivity rate depends on population size through exponential feedback:

$$r(y) = \frac{1}{\tau}\exp(Ky), \tag{2}$$

where τ is a time scale and K is a real parameter that can be positive or negative. The corresponding differential equation reads

$$\frac{dy}{dt} = r(y)\,y = \frac{y}{\tau}\exp(Ky). \tag{3}$$

Here and in the following, y denotes a dimensionless, regime-wise normalized population:

$$y \equiv \frac{N(t)}{N(t_0)}, \tag{4}$$

where t_0 is the start time of the regime under consideration. This regime-wise normalization is used to compare growth curvature across distinct historical intervals and does not imply that the entire 12,000-year record is described by a single globally continuous solution of Eq. (3) with fixed parameters. The above normalization makes the argument Ky dimensionless (hence K is dimensionless).

Eq. (3) allows the productivity rate to increase with y for $K > 0$ or to decrease with y for $K < 0$. In the context of glassy relaxation, a closely related equation appears with a minus sign on the right-hand side [17,18], because it describes decay rather than growth.

Controlled approximations and relation to classical laws

It is important to distinguish controlled local limits from global dynamical equivalence. We do not claim that Eq. (3) is globally phase-space equivalent to the logistic Verhulst equation, nor that it shares the same equilibrium structure. Instead, classical laws arise from controlled truncations of $\exp(Ky)$ in the regime $|Ky| \ll 1$. Malthus is recovered exactly only in the singular limit $K \to 0$: upon linearizing about $Ky = 0$, $\exp(Ky) \approx 1$, Eq. (3) reduces to $\frac{dy}{dt} = \frac{1}{\tau} y$.

For $K < 0$ and $|Ky| \ll 1$, $\exp(Ky) \approx 1 + Ky \approx 1 - sy$ with $s \equiv -K > 0$, yielding the logistic-like truncation $\frac{dy}{dt} \approx \frac{y}{\tau}(1 - sy)$. This approximation is valid only over finite ranges of y where $|Ky| \ll 1$; it is not a statement of global equivalence of the two dynamical systems.

For $K > 0$ and $|Ky| \ll 1$, $\exp(Ky) \approx 1 + Ky$, and Eq. (3) reduces to the Riccati-type quadratic truncation $\frac{dy}{dt} \approx \frac{y}{\tau} + \frac{K}{\tau} y^2$, whose solutions can display von Foerster-type hyperbolic growth under appropriate conditions. Again, this hyperbolic form pertains to the truncated Riccati-type limit and should not be confused with the finite-time divergence of the full Eq. (3).

Malthus. For $K \to 0$ (equivalently $|Ky| \ll 1$ with leading order retained), $\exp(Ky) \approx 1$ and Eq. (3) reduces to $\dot{y} = y/\tau$, i.e. Malthusian growth.

Logistic-like (Verhulst) behaviour as a local truncation. For $K < 0$ and $|Ky| \ll 1$, $\exp(Ky) \approx 1 + Ky \approx 1 - sy$ with $s \equiv -K > 0$, giving a logistic-type truncation $\dot{y} \approx (y/\tau)(1 - sy)$. This is a local approximation valid over finite ranges of y. The long empirical plateaus in Fig. 1 are described phenomenologically by $\beta \approx 0$ in the empirical fits of Ref. [8] and are not claimed to be exact equilibria of Eq. (3).

Riccati/von Foerster as a local truncation. For $K > 0$ and $|Ky| \ll 1$, $\exp(Ky) \approx 1 + Ky$, giving $\dot{y} \approx (y/\tau)(1 + Ky)$, i.e. a Riccati-type growth law whose solutions include hyperbolic behaviour under appropriate conditions, consistent with von Foerster-type fits.

Exact solution and qualitative behaviour

Without truncating the exponential, Eq. (3) admits an implicit solution in terms of the exponential integral Ei:

$$\mathrm{Ei}(-Ky(t)) = \mathrm{Ei}(-K) - \frac{t}{\tau}, \tag{5}$$

with the initial condition $y(0) = 1$. Equivalently,

$$y(t) = -\frac{1}{K}\,\mathrm{Ei}^{-1}\left(\mathrm{Ei}(-K) - \frac{t}{\tau}\right). \tag{6}$$

The hyperbolic divergence arises only in the Riccati-type truncation ($|Ky| \ll 1$); the finite-time divergence follows from the exponential-integral structure and is not globally identical to the Riccati form. For $K > 0$, the exact solution implies a finite-time divergence because $\mathrm{Ei}(-Ky) \to 0^-$ as $y \to \infty$, so that the implicit relation $\mathrm{Ei}(-Ky(t)) = \mathrm{Ei}(-K) - t/\tau$ reaches zero at a finite critical time $t_c = \tau\,\mathrm{Ei}(-K)$. The often-quoted hyperbolic (von Foerster) divergence arises only within the Riccati truncation valid for $|Ky| \ll 1$ and should not be interpreted as the exact asymptotic form of the full solution.

Mapping between β and K

In Ref. [18], a numerical mapping between the Kohlrausch exponent β and the parameter K was obtained for the relaxation-sign convention. An analogous mapping applies here for growth. Using numerical error minimization, we obtain the mapping shown in Fig. 2, which we use to select initial estimates of K for the empirical regimes.

Comparison with empirical regimes

Based on the mapping in Fig. 2, the crossover around 1970 from CEF to SEF corresponds to a change from $K \simeq 0.072$ to $K = -0.032$ in Eq. (3). In Fig. 3(a), we compare the empirical SEF fit for 1970–2023 (Fig. 1) with the numerical solution of Eq. (3) for $K = -0.032$.

In Fig. 3(b) and (c), we analyse two historical CEF regimes. In both cases, the numerical solutions of Eq. (3) are in fair agreement with the empirical CEF fits, with best-fit values $K = 0.062117398$ (panel b) and $K = 0.07227915$ (panel c). Because $K > 0$, the solution exhibits a finite-time divergence.

The orange curves in panels (b) and (c) are best-fit values found by least-squares minimization over $0 < t/\tau < 2$; the blue curves with $K = 0.04$ are shown for illustration. The parameter K is estimated by least-squares minimization against the empirical points over the interval $0 < t/\tau < 2$, which is the range where the empirical curvature of the regime is robust and least affected by regime

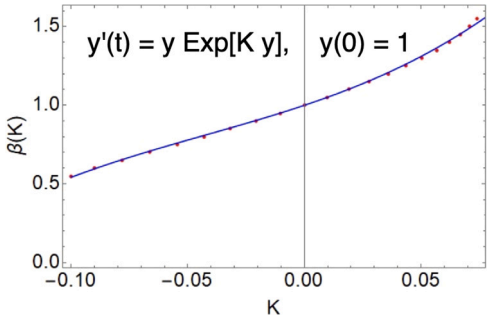

Fig. 2. Mapping between the SEF/CEF exponent β and the parameter K in Eq. (3) obtained by numerical error minimization. Symbols correspond to numerical minimization results; the continuous line is a guide to the eye.

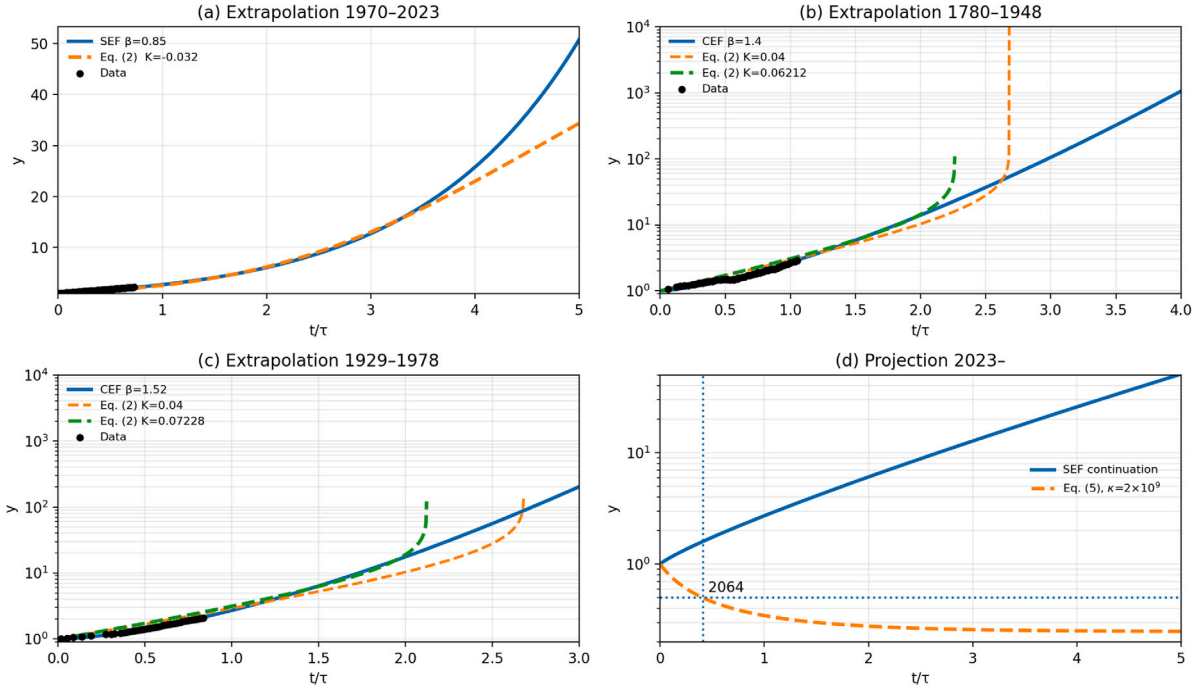

Fig. 3. Extrapolations of global population growth regimes. Markers are empirical data points from Ref. [8] (Appendix table therein), normalized as $y \equiv N(t)/N(t_0)$ and $t \equiv (T - t_0)/\tau$, where T is the calendar year and τ is the characteristic time used in the corresponding SEF/CEF fits [8]. Thus $t = 0$ corresponds to the start year t_0 of the regime. In panels (a)–(c), solid curves are the SEF/CEF fits reported in Ref. [8], while dashed curves are numerical solutions of Eq. (3). Panel (a) (1970–2023): SEF with $\beta = 0.85$, $\tau = 72.7$ yr; Eq. (3) with $K = -0.032$. Panel (b) (1780–1948): CEF with $\beta = 1.40$, $\tau = 160$ yr; Eq. (3) with $K = 0.04$ (illustrative) and $K = 0.062117398$ (best fit over $0 < t/\tau < 2$). Panel (c) (1929–1978): CEF with $\beta = 1.52$, $\tau = 58.6$ yr; Eq. (3) with $K = 0.04$ (illustrative) and $K = 0.07227915$ (best fit over $0 < t/\tau < 2$). Panel (d): projection from 2023, where the solid curve continues the current SEF trend (no carrying-capacity constraint) and the dashed curve shows Eq. (8) if carrying-capacity constraints became abruptly active today. The value $\kappa = 2 \times 10^9$ is a deliberately conservative, worst-case estimate to illustrate the qualitative effect of such a constraint.

crossover. Extending the window further does not qualitatively change the inferred sign of K but increases sensitivity to the onset of the next regime.

To quantify goodness-of-fit in a minimal way consistent with the scope of this work, we evaluate residuals on a logarithmic scale,

$$\epsilon_i = \ln y_i - \ln \hat{y}(t_i), \tag{7}$$

where y_i are the empirical points and $\hat{y}(t_i)$ the model values. We report log-RMSE, log-MAE and R^2 computed on $\ln y$. For the windows shown in Fig. 3 we obtain: (i) panel (a) 1970–2023: log-RMSE = 0.088, log-MAE = 0.083, R^2 = 0.854; (ii) panel (b) 1780–1948: log-RMSE = 0.165, log-MAE = 0.150, R^2 = 0.594; (iii) panel (c) 1929–1978: log-RMSE = 0.181, log-MAE = 0.173, R^2 = 0.254.

Although the fitted values of K are numerically modest, they are not zero and they are dynamically consequential: the sign of K controls whether the growth is stretched ($K < 0$) or compressed ($K > 0$), and the fitted nonzero values reproduce the observed curvature in semi-log representations. If K were negligible, pure exponential (Malthusian) growth would suffice, which is empirically inconsistent with the SEF/CEF regimes analysed here.

Carrying capacity scenario

While the SEF regime with $K < 0$ does not present a doomsday criticality, future developments may lead to a deviation from this trend. A crisis (global conflict, sudden climate acceleration, major epidemic) could reduce the efficiency of resource exploitation and abruptly activate a carrying-capacity constraint. This motivates:

$$\frac{dy}{dt} = \frac{y}{\tau}\exp(Ky)\left[1 - \frac{y}{\kappa}\right], \tag{8}$$

where κ is the Earth's carrying capacity [4]. If the crisis were to set in today, we take $K = -0.032$ (best describing 1970–2023). With a deliberately conservative choice $\kappa = 2\times10^9$ [19–21], Eq. (8) predicts the dashed trend in Fig. 3(d), with a halving of population by 2064. This scenario is approximately compatible with a global population peak around 2030 recently predicted by Yakovenko [6].

Conclusions

Therefore, Eq. (3) provides a compact nonlinear rate-feedback framework that reproduces multiple empirically observed growth regimes as controlled limiting behaviours and/or over the finite historical windows of interest. We are not aware of any other single-rate-feedback ordinary differential equation that captures both stretched- and compressed-exponential curvature through the sign of one parameter K while remaining analytically tractable. Classical laws (Malthus, logistic-like behaviour, Riccati/von Foerster) arise as controlled local truncations, while the full equation captures the observed curvature differences across stretched- and compressed-exponential regimes via the sign and magnitude of K. While the current global population growth trend corresponds to $K < 0$ and does not lead to a doomsday criticality, reverting to an effectively $K > 0$ regime would reintroduce a finite-time divergence in the uncontrolled dynamics. In a separate conservative scenario where carrying-capacity constraints become abruptly active, Eq. (8) predicts a rapid population decline.

CRediT authorship contribution statement

Alessio Zaccone: Writing – review & editing, Writing – original draft, Validation, Methodology, Investigation, Formal analysis, Conceptualization. **Kostya Trachenko:** Writing – review & editing, Writing – original draft, Validation, Formal analysis, Conceptualization.

Ethical statement

This article does not contain any studies with human participants or animals performed by any of the authors. All simulations/analyses were carried out using computational methods; therefore no ethical approval was required.

Declaration of competing interest

The authors declare the following financial interests/personal relationships which may be considered as potential competing interests: Alessio Zaccone reports financial support was provided by University of Milan. If there are other authors, they declare that they have no known competing financial interests or personal relationships that could have appeared to influence the work reported in this paper.

Acknowledgements

This work is dedicated to the memory of my friend and collaborator Prof. Kostya Trachenko who passed away shortly after the writing of this paper. Many useful discussions with Prof. Valeriy Ginzburg and Prof. Oleg Gendelman are gratefully acknowledged. A.Z. gratefully acknowledges funding from the European Union through Horizon Europe ERC Grant number: 101043968 "Multimech", from US Army Research Office through contract no. W911NF-22-2-0256, and from the Niedersächsische Akademie der Wissenschaften zu Göttingen in the frame of the Gauss Professorship program.

Data availability

The empirical population data analysed in this work are taken from Ref. [8] (including its appendix table). No new data were generated.

References

[1] Malthus RT. An essay on the principle of population. London: J. Johnson, in St. Paul's Church-yard; 1798.
[2] Verhulst P-F. Corresp Math Phys 1838;10:113–21.
[3] Lotka AJ. Elements of mathematical biology. New York: Dover; 1956.
[4] Murray JD. Mathematical biology. New York: Springer; 2002.
[5] von Foerster H, Mora PM, Amiot LW. Science 1960;132(3436):1291–5.
[6] Yakovenko VM. Physica A: Statistical Mechanics and its Applications 2025;661:130412.
[7] Perevaryukha AY. Biophysics 2021;66(6):974–91.
[8] Sojecka AA, Drozd-Rzoska A. Sci Rep 2024;14(1):9853.
[9] Kohlrausch F. Pogg. Ann Phys Chem 1854;91:179.
[10] Phillips JC. Rep Progr Phys 1996;59(9):1133.
[11] Ngai KL. The glass transition. New York: Springer; 2011.
[12] Binder K, Kob W. Glassy materials and disordered solids. World Scientific, Singapore; 2011.
[13] Zaccone A. Theory of disordered solids. Cham: Springer; 2023.
[14] Ruta B, Chushkin Y, Monaco G, Cipelletti L, Pineda E, Bruna P, Giordano VM, Gonzalez-Silveira M. Phys Rev Lett 2012;109:165701.
[15] Wu ZW, Kob W, Wang W-H, Xu L. Nat Commun 2018;9(1):5334.
[16] Li Q, Peng X, McKenna GB. Soft Matter 2019;15:2336–47.
[17] Trachenko K, Zaccone A. J Phys: Condens Matter 2021;33(31):315101.
[18] Ginzburg VV, Gendelman OV, Zaccone A. Macromolecules 2024;57(5):2520–9.
[19] Lianos TP, Pseiridis A. Environ Dev Sustain 2016;18(6):1679–99.
[20] Dasgupta P. Time and the generations. New York: Columbia University Press; 2019.
[21] Tamburino L, Bravo G. Ecol Indic 2021;129:107973.